Post-flight Analysis of IRDT Blackout during Earth Re-entry

Philippe Reynier[1]
Ingénierie et Systèmes Avancés, Mérignac, 33702, France

and

David Evans[2]
Fluid Gravity Engineering, St Andrews, Fife, KY16 9NX ,United Kingdom

The IRDT flight performed in 2006 was not nominal. The flight was characterized by a blackout period shorter than expected. Here, two methods are applied to perform a post-flight analysis. The first one, based on an engineering approach, has already been used for the preflight analysis. The second involves coupled calculations between a CFD and an electromagnetic solver. The main objective of this post-flight analysis is to validate this advanced approach using flight data and to assess the validity of the engineering method. Numerical results show that the engineering method overpredicts the blackout duration due to the fact that this method is based on a severe on/off switch. The coupled approach leads to an underestimate of the blackout period. Several uncertainties, such as the influence of ablative material on ionization, could explain this discrepancy. Analysis establishes the validity of the coupled approach but its accuracy depends strongly on the modeling used for the calculations.

Nomenclature

Att	=	signal attenuation in Db
E_z	=	Z component of the electric field in direction of Earth
F_{np}	=	Fourier transform without plasma
F_p	=	Fourier transform in presence of plasma
f_p	=	plasma frequency
f_{link}	=	link frequency
m_e	=	electron mass
n_e	=	electron density
$n_{e,crit}$	=	critical electron density
q	=	electron charge
t	=	time from launch
ε_0	=	permittivity of vacuum

I. Introduction

In the frame of the Manned Spaceflight and Exploration Programme and of the Technological Research Programme of the European Space Agency, several Earth entry orbital demonstrators were developed. Among them, three IRDT (Inflatable Re-entry and Descent Technology) demonstrators[1] were developed in cooperation with EADS and the BSC (Babakin Space Center) in Russia and flown from 2000 to 2005.

The use of an inflatable technology has some impact for the entry analysis. If the inflatable structure is used as a backward braking device, the same phenomenon as for flows around flaps can occur. Like for a flap, the presence of

[1] Research Engineer, ISA, BP 20005, 19 Allée James Watt, 33703 Mérignac, France, Philippe.Reynier@isa-space.eu

[2] Senior Scientist, FGE, 83 Market Street, St Andrews, Fife, KY16 9NX, United Kingdom, David.Evans@fluidgravity.co.uk.

a backward device can induce, some local heating due to the presence of gaps and/or corners, and the flow-field itself can be influenced by strong fluid/structure interactions[2]. The main aspect of the inflatable technology is at the system level; indeed the use of an inflatable device is much more complex than the choice of a rigid heat-shield. Inflation occurs at high altitude and high velocity, and this is a key issue in the absence of a ground test facility capable of reproducing this process in flight conditions.

The last vehicle of the IRDT series, IRDT-2R, was launched successfully on October 7 2005. However, an incident occurred during the flight, most probably due to the bursting of the inflatable device, inducing a non-nominal trajectory and the loss of the capsule which was not recovered. IRDT-2R was equipped with an ARTS antenna of 219 MHz, embedded in the front-shield, in order to ensure communications during the flight except during the blackout period. From the data recovered before the end of transmission from the capsule, the blackout period was found to be also non-nominal.

This paper focuses on the analysis of the blackout duration during the IRDT-2R flight. From the non-nominal trajectory rebuilt at ESTEC, based on the scenario of a deflation of the MIBD (Main Inflatable Breaking Device) during the flight, an analysis of the blackout duration has been undertaken using engineering and advanced approaches. The engineering method, already used for the mission preparation[3], is based on shock layer analysis and correlations. The advanced approach is a coupling between CFD and electromagnetic simulations.

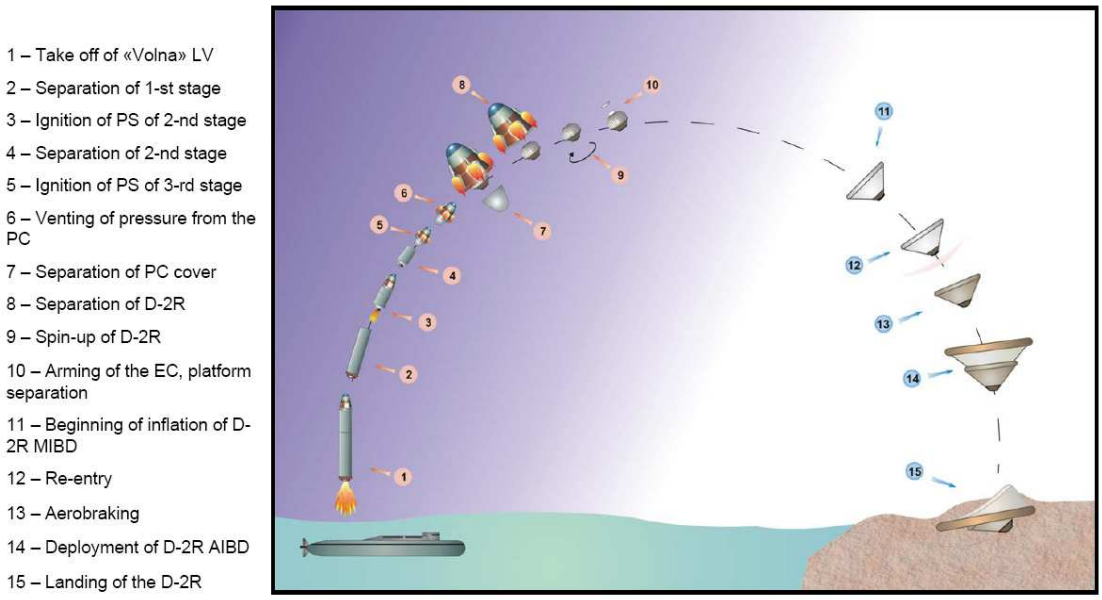

Figure 1: Nominal mission profile of IRDT-2R (credit to Babakin Space Center)[4].

II. Trajectory Analysis

This section describes the mission and in-flight scenarios. The analysis performed at ESA-ESTEC[5], and the trajectory retained for the blackout analysis, are briefly reviewed.

A. Nominal scenario

The nominal scenario of the IRDT mission is shown in Fig. 1. The mission can be summarized as follows. The launch was performed from a Russian submarine in the Barents Sea by a VOLNA rocket. After the separation of the capsule and its spinoff, the entry occurred at 100 km altitude with an entry velocity of 6869 m/s and took place at 60.88˚ latitude North and 159.2˚ longitude East. The re-entry angle was -6.84˚. The inflatable device was in two parts, the MIDB, Main Inflatable Breaking Device, and the AIBD, Additional Inflatable Breaking Device. MIBD deployment was planned to be achieved just before the re-entry while AIBD deployment occurred at a nominal value of 7.5 km. The landing was planned in the Kamchatka peninsula.

During the mission, communications with the ground were ensured through a telemetry antenna system, ARTS (Autonomous Radio Telemetry System), operating in the UHF band with a frequency of 219 MHz. In the mission scenario, the blackout zone was planned to start at the beginning of the re-entry at 100 km of altitude and t= 906.94s

(from launch) and to end at t=986.94 s, so the duration was 80 s. The duration estimated at the Babakin Space Center (BSC) was initially of 60 seconds but a margin of 20 seconds was accounted for[6].

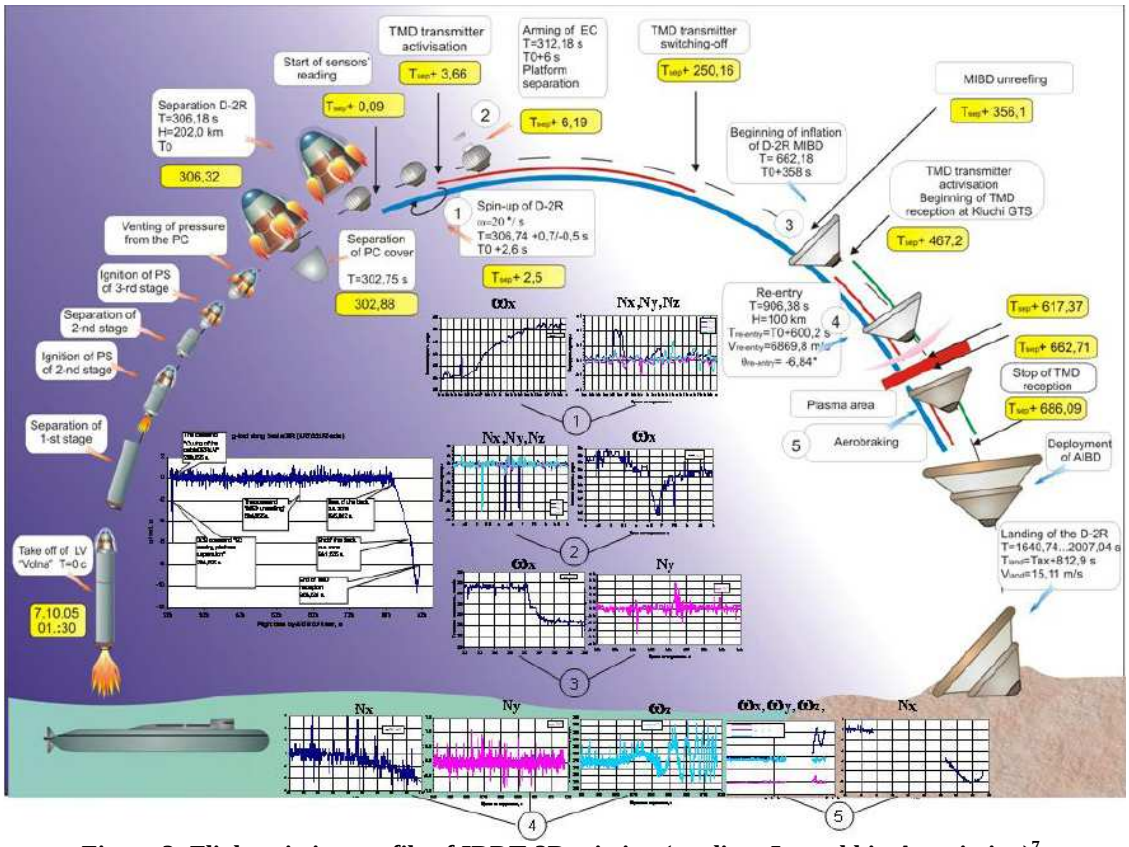

Figure 2: Flight mission profile of IRDT-2R mission (credit to Lavochkin Association)[7].

		MIBD completely deflated	MIBD half deflated	MIBD Almost completely deflated
Nose radius	**[m]**	0.61	0.61	0.61
Base diameter	**[m]**	0.89	1.6	1.1
Reference Area	**[m2]**	0.622	2.04	0.95
Masse	**[kg]**	130	130	130

Table 1: Configurations of the capsule selected for the different scenarios[5].

B. In-flight scenario

The in-flight scenario, summarized in Fig.2, was different from what was expected. The launch was successful as well as the separation of the capsule from the cover, the spin-off and the inflation just before re-entry at t = 906.38 s. The flight was nominal till the beginning of the blackout zone, starting a little bit later than expected, at t = 923.695s from launch. Then, blackout duration was shorter than expected with duration of 45.338 seconds. The telemetry was lost at t=992.41 seconds and today the capsule has not been recovered.

The analysis of the flight data shows that the g-load evolution during the flight was not nominal. The g-load distributions computed at BSC and ESTEC for a nominal flight are compared to the flight data in Fig. 3. There is a slight difference between the trajectory calculated at ESTEC and BSC, with a maximum of g-load predicted 4 seconds earlier than in the BSC's trajectory. This discrepancy might be due to some differences in the atmosphere models used in the calculations. The comparison with the flight data gives good agreement with the nominal predictions before the entry in the blackout region. However, a huge discrepancy is found after the end of the

blackout period, which shows that, if the trajectory was nominal before the blackout zone this was not the case after the end of the blackout.

C. Recovery of flight trajectory

A trajectory analysis has been carried out at ESTEC[5] with the objective of finding a reliable interpretation of the flight data. According to this study, the most reliable explanation for the non-nominal trajectory is the deflation of the MIBD during the re-entry. This is highlighted in Fig. 4 where the g-load distributions computed for different scenarios (MIBD fully deflated, almost completely deflated and half deflated) are plotted. The different characteristics such as the base diameter and the reference area used to compute the trajectory are reported in Table 1. The scenario where the MIBD is almost completely deflated at t=55s (from the beginning of re-entry at 100 km of altitude) fits the best the flight data. Other post-flight trajectory analysis carried out at IRS[8] and BSC[7] arrived at the same conclusions. As a consequence, this scenario, based on the hypothesis of an almost complete deflation of the MIBD during re-entry, has been retained as baseline for the current study on blackout.

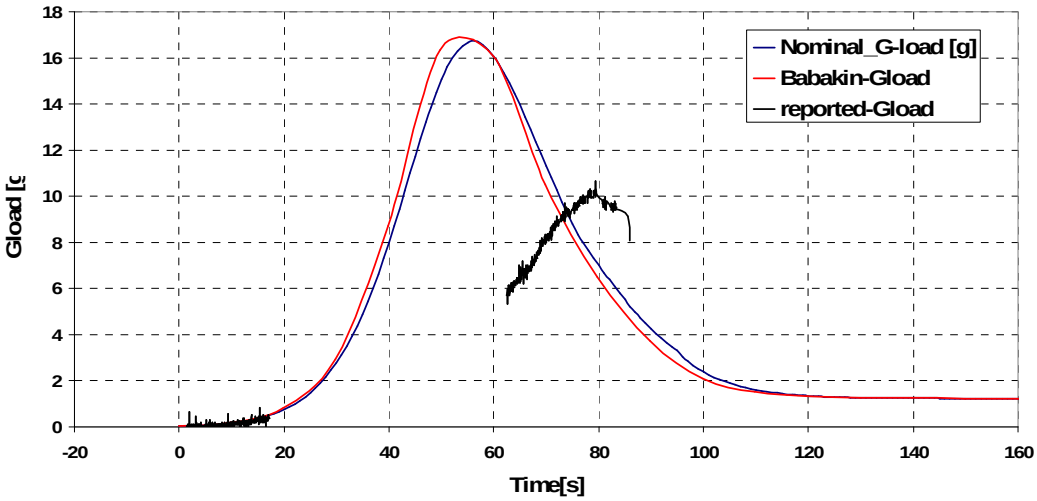

Figure 3: G-load distributions computed at ESTEC (nominal_G-load) and BSC for the nominal trajectory and flight data (reported-Gload) [5].

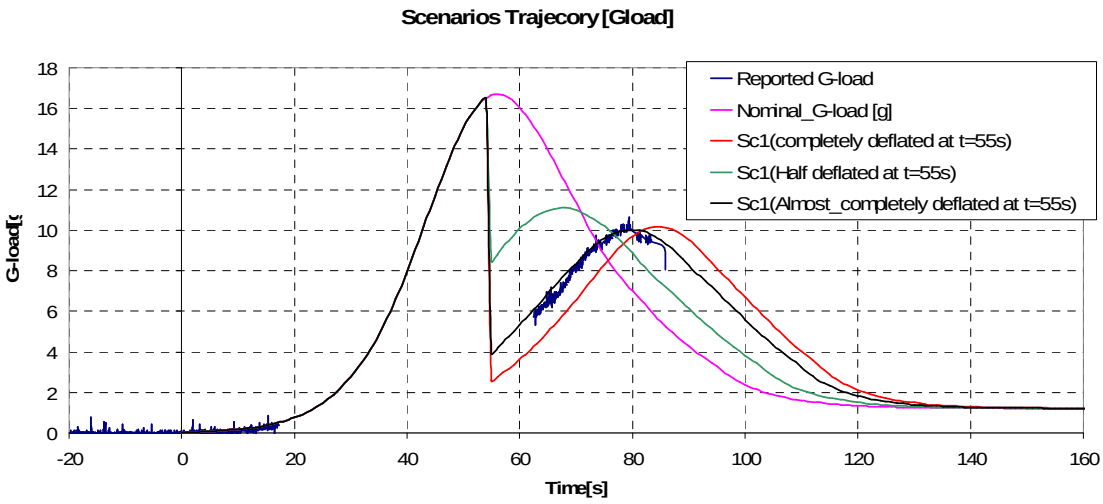

Figure 4: G-load distributions and sensitivity analysis for the deflation scenario.

III. Engineering Approach for Blackout Analysis

A high level of electron density around the spacecraft during the flight induces the blackout phenomenon associated with ionization. When a critical density of electrons for a given frequency is reached the communication is cut. The critical electron densities for the different communication bands[9] UHF, S, X and Ka, are listed in Table 2. During IRDT flight, the communications with the ground were ensured by an Autonomous Radio Telemetry System (ARTS). The ARTS antenna was operating in the UHF band at a frequency of 219 MHz. The antenna, embedded in the heat-shield as shown in Fig. 5, had an annular shape (with the stagnation point as centre) and was emitting forward[6]. This means that the signal emitted by the antenna had to cross the shock wave located upstream of the vehicle front shield. During entry, ARTS was not used during the blackout zone and from a mission point of view, the duration of the blackout period had to be estimated.

Link frequency (GHz)	Designation	Critical Electronic Density (electrons/cm^3)
0.4	UHF Band	$1.99 \cdot 10^9$
2.3	S Band	$6.56 \cdot 10^{10}$
8.4	X Band	$8.75 \cdot 10^{11}$
32.0	Ka Band	$1.27 \cdot 10^{13}$

Table 2: Minimum frequencies and critical electronic densities for different communication bands.

In order to complete the post-flight analysis based on trajectory predictions, a study has been undertaken to reassess previous blackout predictions during the flight as a function of the new trajectory. This has been carried out in two steps. In a first step, an engineering approach, developed and used already for the mission preparation[3] has been applied to the flight trajectory. In a second step, a more advanced method based on coupled simulations between CFD and electromagnetism solvers has been developed.

A. Engineering method

During a re-entry, a high level of electron density around the spacecraft induces the blackout which is associated with ionization. For a preliminary analysis, an in-depth study of the blackout coupled to three-dimensional numerical simulations of the IRDT configuration at different locations during the early stages of the re-entry could not be undertaken. Therefore, an engineering approach was developed to predict the blackout duration.

This method, based on an on/off switch, is described here. Phenomena like diffraction, coupling with radiation and propagation of electromagnetic waves within the plasma are beyond the scope of an engineering study and are not accounted for. Frequency attenuation is also not considered here. In order to assess the blackout duration, the critical electron density for the ARTS frequency has to be determined. When the critical density of electrons is reached the communication is cut. For a given electron density, n_e, the corresponding plasma frequency, f_p, in Hz, is expressed as,

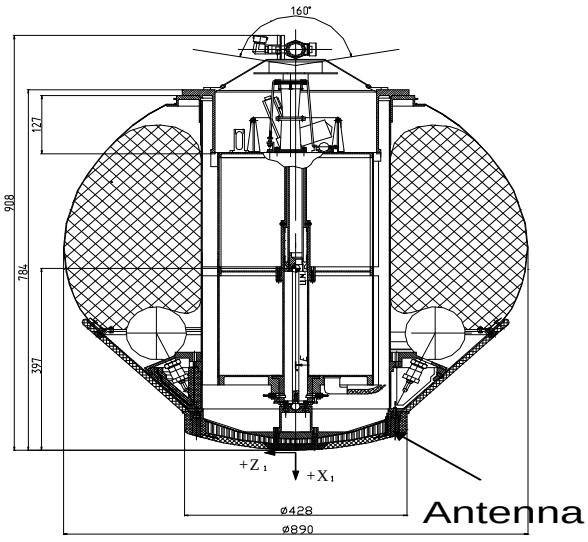

Figure 5: Sketch of IRDT with embedded antenna location.

$$f_p = \frac{1}{2\pi}\sqrt{\frac{q^2 n_e}{\varepsilon_0 m_e}} \quad , \qquad (1)$$

Where, q is the electron charge, m_e the electron mass and ε_0 the permittivity of vacuum. From this equation the critical density, $n_{e,crit}$, for a communication band is given as,

$$n_{e,crit} = \frac{f_{link}^{\ 2}}{80.64 \,.\, 10^6} \quad , \qquad (2)$$

where, f_{link} is the link frequency, expressed in Hz, of the investigated band. Applying this equation to the ARTS frequency, the critical density for this antenna is found to be 0.594×10^9 electrons per cubic centimeter.

In order to predict the electronic density around the TPS, the chemistry composition along the stagnation line has been computed using the shock layer solver, PMSSR[10] for different points of the trajectory. Using this tool an

axisymmetric approach is used to determine the shock layer accounting for chemical and thermal non-equilibrium. Here, an Earth atmosphere thermochemical model[11] accounting for ionization, with 11 species (N_2, N_2^+, N, N^+, O_2, O_2^+, O, O^+, NO, NO^+, e-) and 16 chemical reactions has been used for the calculations. According to Greendyke et al[12], only minor differences can be found between axisymmetric and three-dimensional computations for blackout prediction. In this work, only one thermochemical model is used, while a parametric study[12] has shown a particular sensitivity of the onset and severity of electron avalanche phenomena associated with changes in the thermochemical model. An extension of this study would be to perform a parametric study of the chemistry composition with several thermochemical models.

Using this methodology, the electronic density is computed with PMSSR along the stagnation line and compared to the critical densities for the antenna. Then a first estimate of the blackout duration can be performed since the antenna is close enough to the stagnation point.

B. Pre-flight Analysis

Using this methodology, in order to prepare the mission[3], the electronic density has been computed and compared to the critical densities for the ARTS and the different frequency bands reported in Table 2 for predicting the mission blackout duration.

Several computations have been made for different times of IRDT entry, from t = 906.94s to t = 971.94s. The calculations have been stopped when the electron density was lower than the critical density for the ARTS frequency. The electron density has been computed along the stagnation line, since the antenna is embedded in the front shield. The electron density at the antenna location and at the stagnation point should be of the same order. In Fig. 6, the electronic densities, computed for different points of the trajectory, are plotted as well as the critical electron densities for different bands. Results show that the critical density for the Ka band is reached at t = 966.94 s that corresponds to the peak of heat-flux during the entry. It is also the moment of entry with the highest ionization effects. The blackout duration lasts only a few seconds in this band. The blackout duration for X and S bands is close to 35 and 50 seconds respectively. For the frequency of interest here, the ARTS frequency, blackout is longer. According to our numerical results, it lasts 60 seconds.

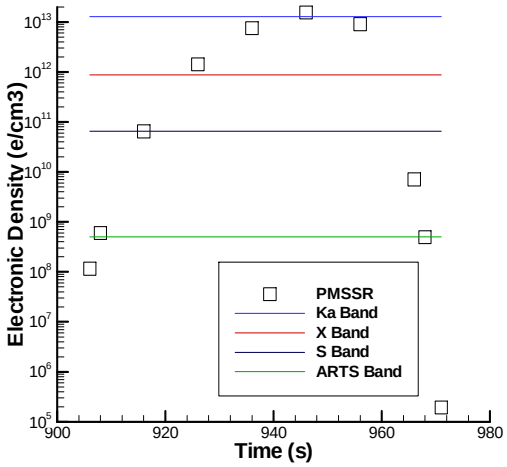

Figure 6: Evolution of the electronic density during IRDT entry. The lines correspond to the critical density for Ka, X, S and ARTS bands.

The blackout duration during the IRDT mission has also been estimated at BSC[6]. According to this work, the blackout zone lasts from the start of re-entry at t = 906,94 s to t = 986,94 s. This was longer than the predictions with, at first sight, a discrepancy of 20 seconds. However, for the mission preparation a margin of 20s was considered for the entry beginning and this margin was integrated in the blackout duration. This explains this apparent discrepancy between the blackout duration considered for the mission design and the predictions performed with the engineering method. In fact, the blackout duration estimated by BSC was 60 seconds from the maximum time of the entry beginning, so finally in very good agreement with the predictions performed at ESTEC.

C. Post-flight Analysis

In order to estimate the reliability of the engineering approach developed for the mission analysis, it is of interest to apply it for the post-flight analysis. This has been done during the re-entry from t = 0 s to t = 80 s for the trajectory corresponding to the scenario with an almost completely deflated MIBD shown in Fig. 4. From the trajectory derived using the flight data, the electron densities computed along the stagnation line have been computed and compared to the critical density for the ARTS band. Fig. 7 shows the flight data with the g load distribution, the electronic density computed at the stagnation point and the critical electronic density for the ARTS band. The beginning and end of the blackout zone are also reported in this figure. During the flight, the blackout zone lasted from t = 17.315 s to t = 62.65 s from the re-entry time, so lasting 45.3 s, which is less than expected during the mission preparation.

The beginning of the entry is nominal and as for the mission preparation, the computations predict the beginning of the blackout zone at t = 7 s after re-entry. The blackout zone is expected to last until t = 75 s, therefore 12.4 s after the end of the blackout zone during the flight. Then, the engineering method predicts the onset of blackout 10.3 s

earlier and the end 12.4 s later that the flight data. The duration of the blackout zone is overpredicted by 22.7 s: a blackout duration of 45.3 s during the flight compared with 68 s in our computations.

The discrepancy between the predictions and the flight data can be explained by several factors. A previous study[12] has established a particular sensitivity to the onset and severity of an electron avalanche phenomenon associated with changes in the thermochemical model. Such a fact could explain the discrepancy in the onset of the blackout predictions but not for the end of the blackout zone. Another point is the approach itself that might be too elementary to handle such a phenomenon, indeed this engineering method is a rather severe on/off switch. An extension of this study could be to perform a parametric study of the chemistry composition with several thermochemical models. A possibility to refine the approach would be to use electron densities predicted by CFD computations. The present analysis neglects also the ablation process that could create species increasing or decreasing the level of ionization in the shock layer. In order to provide a better assessment of the blackout period, in the next section coupled calculations will be performed using CFD and electromagnetic solvers.

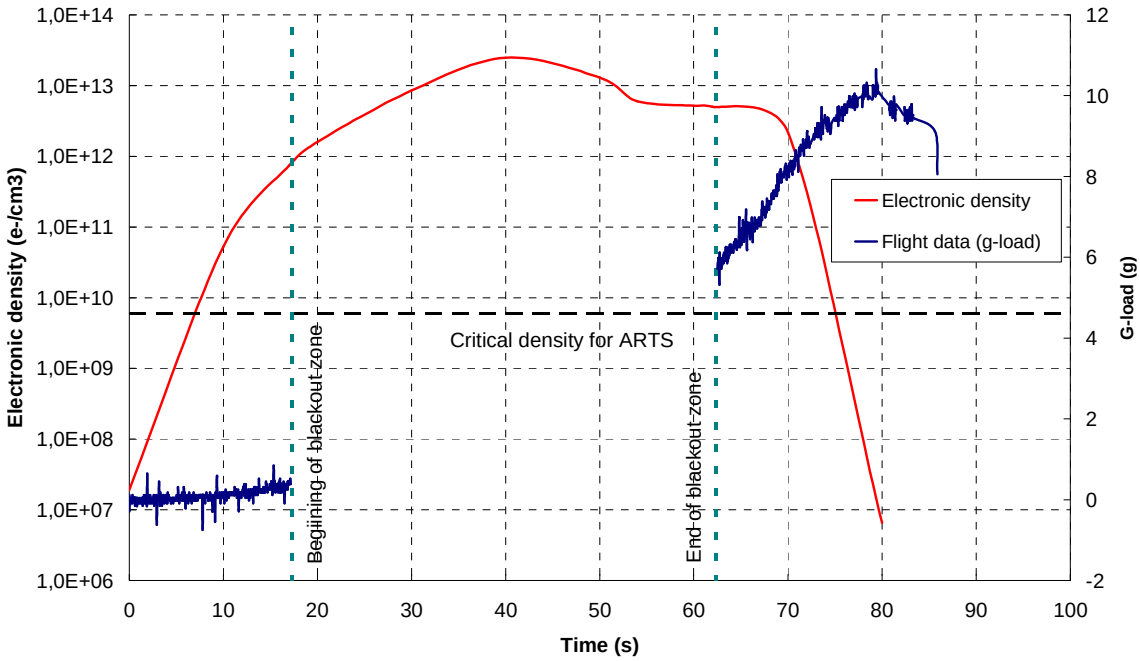

Figure 7: Evolution of the electronic density during IRDT entry and flight data for the g load. The horizontal line corresponds to the critical electronic density for the ARTS band.

IV. Coupled Approach

In order to refine the results obtained using the engineering approach and also to assess its reliability, a coupled approach has been applied to the problem. This blackout analysis is based on the coupling between the numerical simulations performed using TINA[13] which are post processed using a suite of codes. The method is described hereafter.

A. CFD Predictions

During a re-entry, the high level of electron density around the spacecraft induces the blackout which is associated with ionization; as a consequence the numerical simulations performed with TINA have been performed accounting for

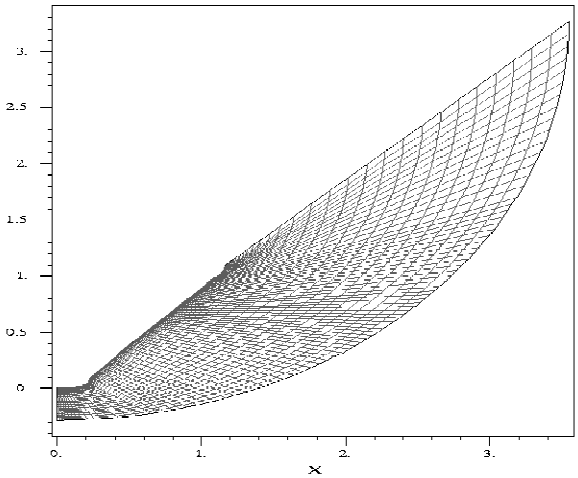

Figure 8: Mesh used for the computations.

this phenomenon. In this objective, the thermochemical model proposed by Park[11] has been retained. This is an 11 species model (O_2, N_2, O_2^+, N_2^+, O, O^+, N, N^+, NO, NO^+, e^-) with 16 chemical reactions. Computations have been performed without surface catalysis: since the maximum of the electron population is close to the shock location, their mass fraction at this location should not be modified by catalytic boundary conditions.

Axisymmetric computations have been performed without angle of attack for the capsule. During the flight there was a small angle that has been neglected here. The axisymmetric mesh used for the calculations is 85 × 50 cells mesh and is plotted in Fig. 8.

Trajectory	Time from re-entry (s)	Velocity (m/s)	Altitude (km)	Density (kg/m^3)
Nominal	43	5800	66	$2.\cdot10^{-4}$
Flight	17	6860	85.8	$7.23\cdot10^{-6}$
Flight	63	3355	50.6	$8.\cdot10^{-4}$

Table 3: Characteristics of the trajectory points investigated.

Numerical predictions have been performed for the trajectory points reported in Table 3. First, computations have been carried out for the point of the nominal trajectory corresponding to peak heating conditions. This point is in the strongest part of the blackout region and this calculation is used to test the suite of codes. Then, numerical simulations have been performed for the start and end points of the blackout region observed during the flight, so for the point at 17s and 63s after re-entry.

A TINA prediction is shown in Fig. 9 where the mole fraction of electrons is plotted and the corresponding mass fraction is shown in Fig. 10. This solution was obtained for the trajectory point corresponding to the maximum of heat-flux along the nominal IRDT trajectory[14].

Computations have been performed using some modifications in the calculation of the ambipolar diffusion. The low limit for this quantity has been reduced from 10^{-9} to 10^{-19}. This modification of the ambipolar diffusion assumption for small number densities has been done to avoid a high (erroneous) electron density in the free stream. The calculations were also performed with a very low level of the inflow mass fraction of electrons: 10^{-20}. If a very low mass fraction is not used at the inflow this may result in a too high electron density in the whole field.

The predictions for the two other trajectory points of Table 3 have been

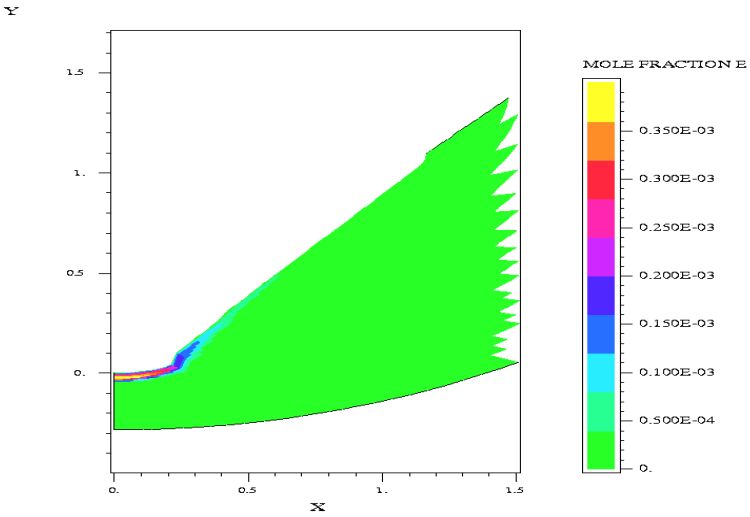

Figure 9: Mole fraction of electrons at peak heat-flux of the nominal trajectory.

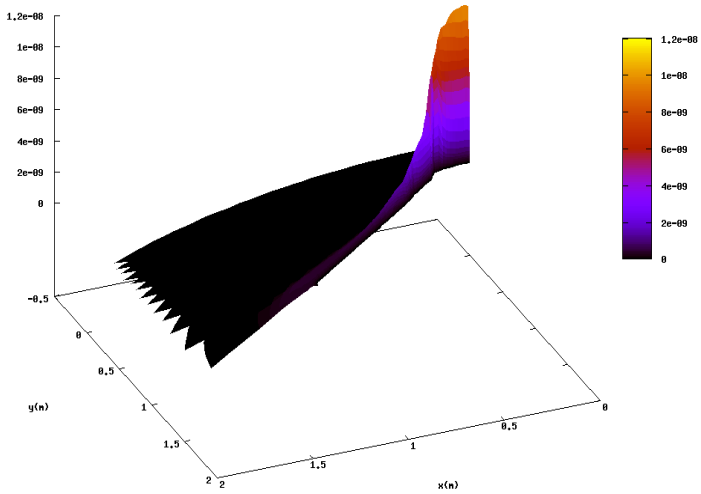

Figure 10: Electron mass fraction at peak heat-flux of the nominal trajectory.

achieved using the same computational conditions.

B. Methodology

First, the results from TINA (2D mesh, electron mass fraction, electronic temperature and density) are mapped to a 3D orthogonal mesh using the link code FLING[15]. The 3D mesh used in FLING includes the entire re-entry vehicle. It is 180 cells along the x and z directions and 108 cells along the y direction, the domain extends from -3 m to 3 m in the x and y directions and from -1 m to 2.6 m in the y direction.

The same tool computes the electron collision frequency and the plasma frequency in each cell of the mesh. Then, the Maxwell equations are solved for the electric field corresponding ARTS transmission through the plasma flow using the electromagnetic solver PLASMA[15].

In PLASMA's input, the antenna location and characteristics have to be provided. Here; the antenna has been located in the cell as close as possible to the real configuration shown in Fig. 5. Because the PLASMA code works in the time domain, it is more convenient to use a broadband Gaussian pulse instead of the 219 MHz antenna signal since sinusoidal pulses do not provide very good results.

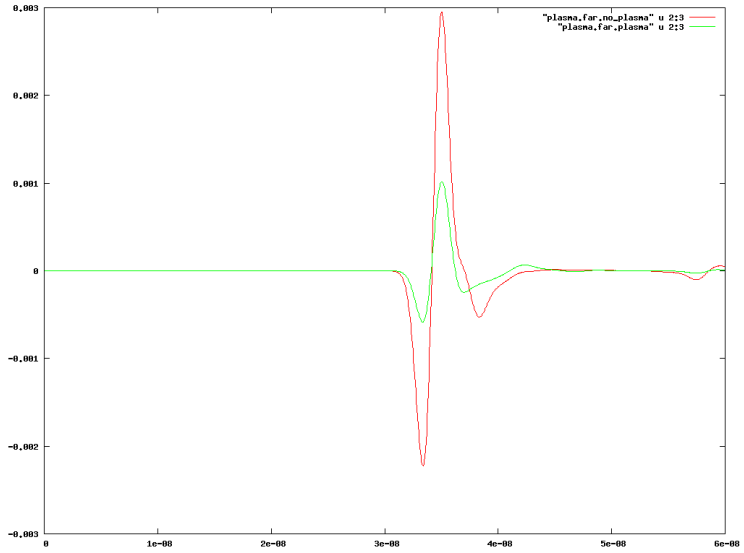

Figure 11: Signals received on Earth with (green) and without (red) plasma attenuation

For assessment of the blackout duration during re-entry, the PLASMA output to be post processed is the one corresponding to the "far-field" which corresponds to what is seen by the receiver on Earth. The measurement of E_z (Electric field in the z direction) is sufficient. To estimate the blackout, the following approach has been adopted. First the electric field for the antenna has to be generated from the vehicle nose. This is done by driving a current in a cell near the antenna. Next, the code PLASMA has to be run again but without plasma. This gives an un-attenuated signal that we can use to compare and thus calculate the attenuation.

Fig. 11 shows the signals seen by the receiver on Earth for the plasma and no plasma runs. The signal is a derivative of the Gaussian pulse having been tranmitted through what is in effect a dipole antenna. The attenuation is easily seen. There is a second small signal seen at the end of the run. This is due to a reflection off the back of the computational mesh which is not physical.

The last step is to obtain the attenuation for the receiver on Earth measured in dB. For this, both outputs from PLASMA are post processed using a Discrete Fourier Transformation (DFT). When the Fourier transform is done the last 10 nanoseconds from the file are cut since they only include the physically meaningless reflection

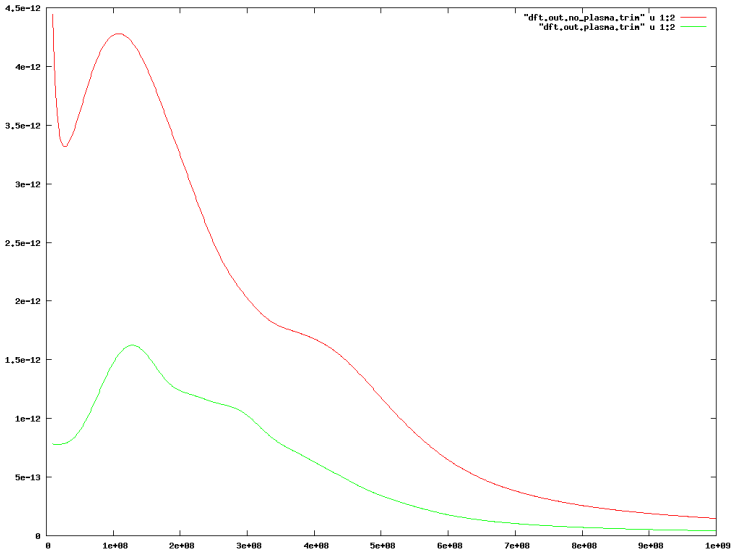

Figure 12: Fourier transforms of the calculations with (green) and without (red) plasma as function of the frequency.

from the PLASMA mesh boundary. The minimum and maximum frequencies required for the calculations using the DFT tool[15] have been set to 10 MHz and 1000 MHz.

The results obtained after the Fourier transformation, with and without the plasma, are plotted in Fig. 12. This figure shows a strong attenuation of the signal under the plasma effects.

The final step is to calculate the attenuation itself. For that the results of Fig. 12have to be converted to the loss of the signal power in decibels (dB) as described hereafter.

If F_p is the Fourier transform of the plasma result and F_{np} the Fourier transform of the no plasma result then the attenuation Att in dB is given by,

$$Att = 20 \log \frac{F_p}{F_{np}} \quad . \qquad (3)$$

The results displayed in Fig. 13 show a plasma attenuation of about 9 dB for the ARTS antenna frequency. A dish antenna of the type that might be used on the ground and used at low frequencies (~1GHz) typically has a gain of around 15 dB. Hence, this loss of 9 dB might not be enough to explain the loss of communications since there could still be some net gain in the communications link. There is however an issue with the mesh dependence of the results. Usually one wavelength should be spanned by 8 to 10 cells. Here the wavelength is 0.73 m which means that the mesh should be sufficient since the cells are 3.33cm per side. However, the plasma zone is only 10 cm wide so this is covered by only 3 cells. This might lead to significant loss of information on the shock plasma.

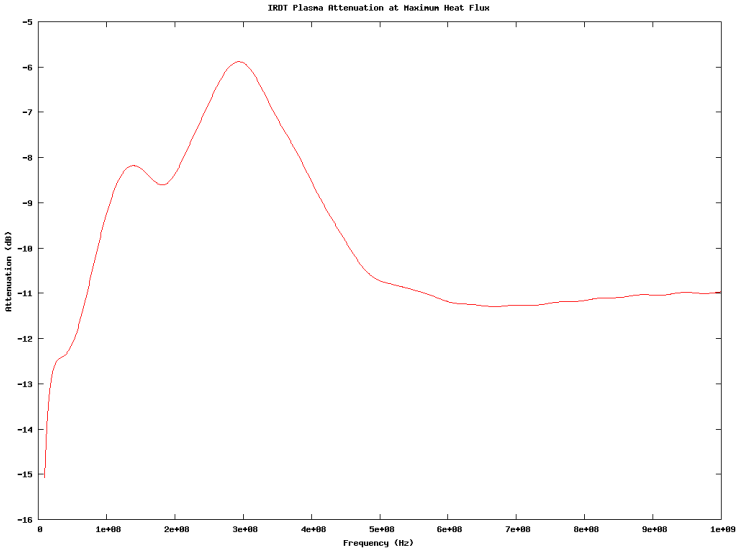

Figure 13: IRDT plasma attenuation in dB as function of the frequency.

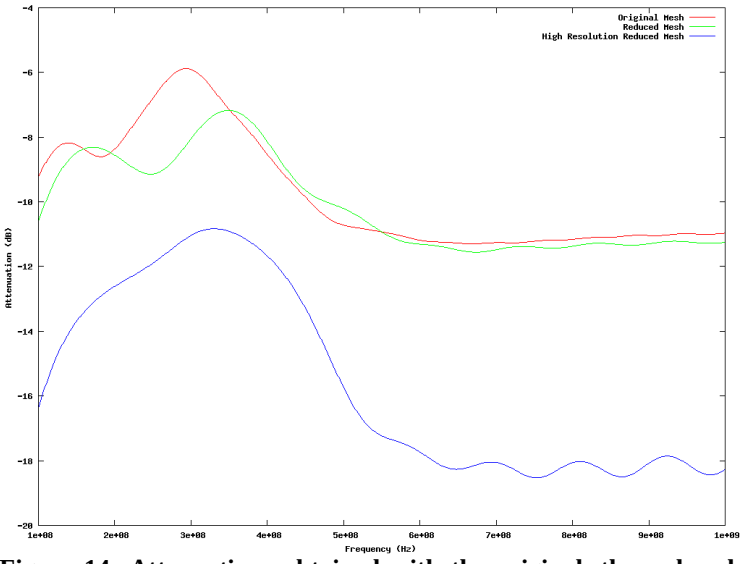

Figure 14: Attenuations obtained with the original, the reduced and the high resolution reduced meshes.

Therefore other runs have been carried out by using a reduced domain extending in the x and y directions from -1.8 m to 1.8 m with 108 cells and from -0.5 m to 1.8 m in the y direction with 69 cells. Then, a more refined mesh has been used on the same domain with 360 cells in the x and z directions and 230 along y. With this last mesh the cells are only 1cm.

The attenuations calculated for the different meshes are plotted in Fig. 14. There is little difference between the two first meshes since the cell sizes are not very different. The reduction in coverage of the PLAMSA mesh does not seem to affect the results in any significant way. Thus we can concentrate on just the nose section of the vehicle and use a higher resolution. With the high resolution mesh the attenuation computed is around 14 dB. This loss of 14 dB almost cancels out the gain of the receiving antenna and so this is likely to be enough to lose communication. However, more information on the communications link to confirm this result would be necessary.

In order to assess the blackout duration during IRDT re-entry, this coupled method has been applied and calculations have been performed for the trajectory points corresponding to the beginning and the end of the blackout zone (see Table 3).

C. Blackout estimation

Numerical simulations of the flow-fields around the IRDT capsule have been carried out for the beginning and end trajectory points of the blackout region. The numerical results have been coupled to the Maxwell solver using the high resolution mesh. The signal attenuation for the beginning point of the blackout period is shown in Fig. 15. The attenuation computed for the beginning point at the ARTS frequency is 17 dB, this value is high enough to fit with the beginning of the blackout zone observed during the flight if we consider a critical value of 15 dB for a dish antenna with a frequency lower than 1 GHz. Moreover, the onset of blackout is very rapid due to the phenomenon of electron avalanche at the beginning of entry when the capsule enters in the first layers of the atmosphere.

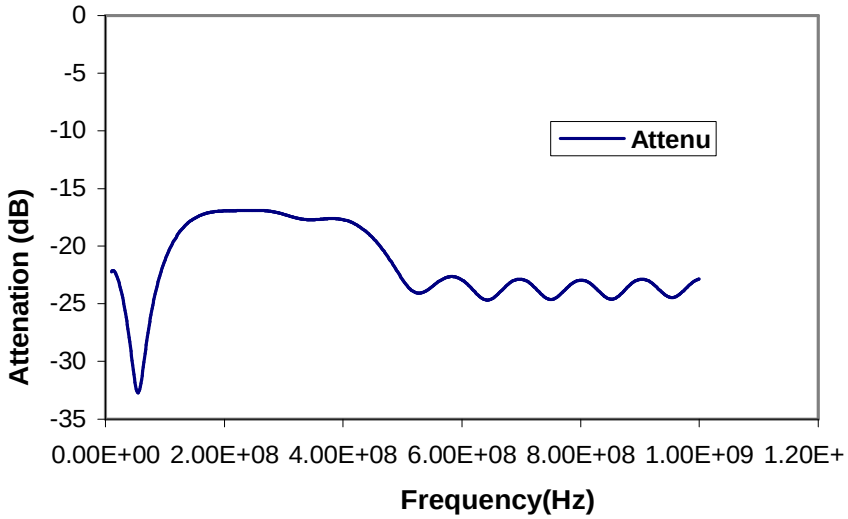

Figure 15: Plasma attenuation computed for the beginning point of the blackout region

The attenuation computed for the end point is plotted in Fig. 16. The attenuation is around 12 dB for the link frequency. This level seems to be a little bit low but since the antenna frequency is much lower than 1 GHz, this level of attenuation might be sufficient to predict the end of the blackout region. More accurate predictions would require additional knowledge of the communications link budget. This is difficult since there is little information available on this point.

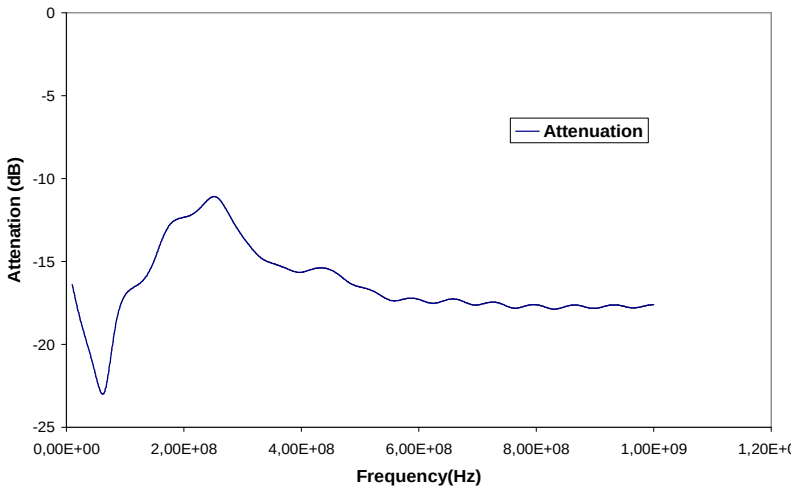

Figure 16: Plasma attenuation computed for the end point of the blackout region.

Now, let consider the critical values for the transmission to the ground station. During re-entry, IRDT is tracked by the "Lyzyk" ground station[14]. According to the Babakin Space Center[14], for this communications link, the ground station can receive the spacecraft signal when the attenuation of the signal is higher than -118.8 dB. The signal received by the station for the period corresponding to the beginning to the end of the blackout zone is from -95 dB to -93 dB. The calculated attenuation is -17 dB at the beginning and -12 dB at the end. Adding these attenuation figures to numbers above, we get values of -112 dB at the beginning and -105 dB at the end. Comparing to the station sensitivity of -118.8 dB, this should still be detectable at the ground station. The information provided[14] is only given for a few points along the trajectory and is only valid for the nominal trajectory. There may be some variability between the points given and the actual sensitivity for the end point of the blackout zone.

Overall, the effects of the plasma are suspected to be underestimated in this study. The method is sound but depends critically on getting the correct estimate of the electron density. This means using a more optimal mesh

around the vehicle and including any effects that may change the ionisation such as the chemistry model or the effects of ablation. This last point is important since the injection of material species in the shock-layer, such as sodium that is used in the fabrication process of some TPS materials[16], can significantly increase the electron density.

V. Conclusion

A post-flight analysis of the blackout duration of the IRDT re-entry has been carried out. First an engineering method, already applied for the mission preparation, has been used. This approach is based on a shock layer prediction tool coupled to the critical antenna frequency for the electron density. This has been able to predict a blackout region including the one observed during the flight.

Then, a coupled approach between CFD and Electromagnetic solvers has been developed and applied to the post-flight analysis. Computations have been performed for the beginning and end points of the blackout region. The results show a lower level of attenuation than necessary for the ground station sensibility. The agreement seems to be acceptable for the beginning point but the station should still be able to receive the signal from the spacecraft at the end.

The two methods used both have problems. The engineering model assumes a one dimensional shock and probably overestimates the electron density. The application of this to determine transmission is basically an on-off switch which is a rather severe assumption. The coupled CFD approach needs a lot of care to ensure that all the important physical features are accurately modelled: optimised mesh, high resolution, and chemistry model, including all ionisation factors. The ablation products from the TPS pyrolysis are not considered in this study. Depending on the TPS composition and blowing efficiency in the shock-layer, these products might have a strong influence on the shock-layer composition and therefore on the electron density. This phenomenon could explain by itself some of the differences between the attenuation predicted and the critical sensitivity of the ground station. The usefulness of the two methods has been demonstrated in this study but their accuracy is still in question.

Acknowledgments

This work has been supported by the European Space Agency through ESA Contract 16666 CCN4/2006. The authors of this paper would like to thank Mr. Arthur Smith from Fluid Gravity Engineering and Dr Lionel Marraffa from ESA/ESTEC for their valuable advices and suggestions.

References

[1]Marraffa, L., Kassing, D., Baglioni, P., Wilde, D., Walther, S., Pitchkhadze, K., and Finchenko, V., "Inflatable Re-Entry Technologies: Flight Demonstration and Future Prospects", *ESA Bulletin*, Vol. 103, pp. 78-85, August 2000.

[2]Mack, A., and Schäfer, R., "Fluid structure interaction on a generic body-flap model in hypersonic flow", *Journal of Propulsion and Rockets*, Vol. 42, pp. 769-779, 2005.

[3]Reynier, P., and Marraffa, L., "Aerothermodynamics investigations for Earth orbital entry vehicles", *Proceedings of the 4th International Symposium on Atmospheric Reentry Vehicles and Systems*, Arcachon, France, March 21-23, 2005.

[4]Babakin Space Center, "IRDT-2RE-Flight Mission: Summary Analysis Report", BSC-IRDT2R-SAR-0001, Babakin Space Center, Moscow, Nov. 2003.

[5]Boutamine, D. E., Marraffa, L., Mazoué, F., and Reynier, Ph., "IRDT Trajectory : Reconstruction of flight data", *Presentation at ESA-ESTEC*, Nov. 11, 2005.

[6]Babakin Space Center, "IRDT-2RE-Flight Mission: Design Defination Report", BSC-IRDT2R-DDR-0004_Rev4, Babakin Space Center, Moscow, Feb. 03. 2005.

[7]Lavochkin Association and Babakin Space Center, "IRDT-2R; Final presentation", ESA-ESTEC, Feb 17, 2006.

[8]Gräßlin" M. H., "IRDT-2R Reentry trajectory Post flight evaluation", IRS Stuttgart, Final presentation, ESA-ESTEC, Feb 17, 2006.

[9]Morabito" D. D., "The spacecraft communications blackout problem encountered during passage or entry of planetary atmospheres", IPN Progress Report 42-150, Jet Propulsion Laboratory, 2003.

[10]Dubois, J., and Smith, A. J., "Program PMSSR V4.1: Inverse shock layer solution with non-equilibrium thermochemistry", TN 132/92-Issue 3, Fluid Gravity Engineering, Emsworth, United Kingdown, Aug. 2004.

[11]Park, C., "Review of chemical-kinetic problems of future NASA missions, I: Earth entries", *Journal of Thermophysics and Heat Transfer*, Vol. **7,** N°3, pp. 385-398, 1993.

[12]Greendyke, R. B., Gnoffo, P. A., and Lawrence, R. W., "Calculated electron number density profiles for the aerossist flight experiment", *Journal of Spacecraft and Rockets*, Vol. 29, N°5, pp. 621-626, 1992.

[13]TINA Version 4, "Theory and User Manual", TN 89/96 Issue 6, Fluid Gravity Engineering, Emsworth, United Kingdom, January 2007.

[14]Babakin Space Center, "IRDT-2RE-Flight Mission: Summary Analysis Report", BSC-IRDT2R-SAR-0001, Babakin Space Center, Moscow, Nov. 2003.
[15]Reynier, Ph., and Evans, D., « PLASMA-FLING User Manual », TN 01V2-2007, ESA-Contract 16666 CCN4/2006, Ingénierie et Systèmes Avancés, Mérignac, France, July 2007.
[16]Jenniskens, P., Wercinski, P., Olejniczak, J., Allen, G., Desai, P. N., Raiche, G., Kontinos, D., Revelle, D., Hatton, J., Baker, R. L., Russell, R. W., Taylor, M., and Rietmeijer, F., "Preparing for Hyperseed MAC: an observing campaign to monitor the entry of the Genesis sample return capsule", Earth, Moon, and Planets, Vol. 95, pp. 339-360, 2004.